

Small-Scale Variation in Snowmelt Energy in a Boreal Forest: An Additional Factor Controlling Depletion of Snow Cover?

JOHN W. POMEROY¹, SUSANNE HANSON¹, AND DEREK FARIA²

ABSTRACT:

Snow ablation and snow cover depletion beneath a forest canopy were investigated at the fine to stand scale, first by theoretical considerations and modelling and secondly using fine-scale measurements of changes to snow water equivalent (SWE) as an indicator of melt energy and of ablation. Three primary differences between observed areal snow ablation and snow cover depletion and calculations that presume uniform snow and energy were investigated:

- 1) spatial variation in initial snow mass,
- 2) spatial variation in melt energy,
- 3) spatial covariance between melt energy and initial snow mass.

A theoretical analysis showed that all three effects can result in areal ablation rates being smaller than available melt energy and contribute effects that cause snow cover depletion curves similar to those that are frequently observed. Field data from a dense boreal spruce stand in the Yukon Territory showed that the spatial distribution of snow water equivalent was lognormally distributed and independent of the energy available for melt, which was normally distributed. Though the spatial variation in melt energy was significant in this forest, ablation calculations that used a synthetic distribution of snow water equivalent and presumed uniform melt energy were sufficient to describe snow cover depletion rates and snow ablation.

Keywords: snowmelt, boreal forest, snowcover depletion, ablation, normal distribution, lognormal distribution, hydrological modelling

INTRODUCTION

The duration and magnitude of snowmelt characterise the spring freshet – normally the peak annual hydrological event in the boreal forest. The apportionment of meltwater to infiltration or runoff and the magnitude of peak flows are strongly associated with the timing and rate of depletion of snow cover. However redistribution of snowfall by interception and variation to melt energetics associated with the forest canopy and stems create an extremely heterogeneous environment for melt processes. Depletion of snow-covered area during melt in forest environments affects areal albedo, sub-canopy energy balance, soil moisture recharge and runoff generation. Buttler and McDonnell (1987) noted that the rate of depletion of snow cover in forest stands can be influenced by the variabilities in snow accumulation or melt rate or some combination of the two. Shook (1995), Donald et al. (1995) and Pomeroy et al. (1998) showed that the distribution of snow accumulation controls the rate of snow cover depletion in open

¹ Centre for Glaciology, Institute of Geography and Earth Sciences, University of Wales, Aberystwyth, Ceredigion, Wales, United Kingdom SY23 3DB wpp@aber.ac.uk

² Water Resources Division, Indian and Northern Affairs Canada, Yellowknife, NWT, Canada

environments. Faria et al. (2000) showed that sequence of snow cover depletion under forest canopies could be partially explained by mean melt rate, spatial distribution of snow water equivalent and association between snow accumulation and energy available for melt.

At sub-stand scales, Woo and Steer (1986), Jones (1987) and Sturm (1992) showed that SWE increases with distance from evergreen tree trunks (up to a distance of roughly three metres) in cold climate forests. Absorption of short-wave radiation by trunks and branches and its redistribution as long-wave energy to adjacent snow may affect the distribution of melt energy at this scale (Golding and Swanson, 1986; Verry et al., 1983; Woo and Geisbrecht, 2000). Shallow snow near to tree trunks may also have a lower albedo (Davis et al., 1997) and leaf litter on the top of forest snowpacks lowers the albedo and increases net radiation to the snow (Hardy et al., 2000).

Shook and Gray (1997) demonstrated that the contribution of additional advected energy from snow-free surfaces during snowmelt decreases with distance from the snow cover edge – though developed for open environments, these principles presumably apply to some degree to a forest environment. Where SWE increases with distance from trunks, then either radiation or advection from trunks or bare ground surrounding trunks could produce an inverse association between SWE and melt energy. Jones (1987) developed a regression equation based on extensive field data that described the influence of proximity to, and size of conifers on SWE. SWE declined with proximity to trunks. The relationship persisted throughout melt, suggesting that melt rates were not significantly higher for greater SWE. Buttle and McDonnell (1987) found that a relationship (admittedly arbitrary) in which melt rate decreased with increasing SWE performed well in predicting snow cover depletion in certain southern Canada forest environments.

Despite the wide range of studies of snowmelt in mid-latitude forests there are no known studies of the variability of snowmelt in high latitude closed canopy forests. Differences from more temperate environments and from open woodlands in the sources and magnitudes of energy for snowmelt may cause different manifestations of the melt and depletion processes.

The objectives of this paper are to:

1. provide initial descriptions of the spatial variability of melt energy and snow water equivalent in a high latitude boreal forest, and
2. show the influence of variability in melt energy and snow water equivalent on rates of snow ablation and snow cover depletion.

THEORY

Melt energy, M is defined as melt energy applied per unit area of snowcover and given in equivalent units of mm SWE, while ablation, A is defined as melt of snow per unit area of ground (mm SWE). Limiting snowmelt by available snow mass per unit area, S , results in

$$A = \min(M, S_s) f_s \quad (1)$$

where f_s is fractional snow-covered area and S_s is SWE per unit area of snow. For this simple and often employed procedure, the fractional area f_s is essential in calculating ablation rates from a sub-canopy energy balance.

If M and S are variable over some spatial coordinate x (that includes non-snow-covered locations) and S is SWE per unit area of ground then

$$A = \int \min(M(x), S(x)) dx \quad (2)$$

In this situation, the spatial distributions of M and S are important, as is any association between M and S (e.g. Faria et al., 2000). In iterative calculations over time, such as used in many models, subsequent values of both A and f_s depend on the proportion of locations where $M > S$; calculation procedures for f_s from situations where S varies with x are shown by Faria et al. (2000). Derived from Eq. 2, f_s is not only used to calculate albedo and advection, but the infiltration of meltwater to frozen soil.

Shook (1995) showed that S can be fitted to a two-parameter lognormal frequency distribution where

$$S = \bar{S}(1 + K CV) \quad (3)$$

and CV is the coefficient of variation and K is the frequency factor calculated from the rank of observation and based upon a linearisation of the probability density function.

Theoretical Simulations

As an example of Eqs. 1–3, five types of spatially distributed ablation simulation were calculated, each simulation starting with 50 mm S_i (initial snow accumulation) and complete snowcover ($f_s=1$), and is given an average M of 10 mm per melt period. The assumptions governing the simulations are described in Table 1. In simulation A, both M and S are uniform over space (Eq. 1); this is similar to the formulations used in many hydrological and climatological models. In simulation B, the two-parameter lognormal distribution describing S_i (Eq. 3) has been supported by a number of studies (Pomeroy et al., 1998); a typical coefficient of variation of S_i and K values from 2.5 to -2.5 were used to generate the distribution. Normally distributed M values were randomly and independently applied to each location for each melt period in simulation C; the distribution and its coefficient of variation anticipate the results shown later in this paper. The function describing positive covariance in simulation D is arbitrary and designed so that mean melt energy remains at 10 mm for each period. The function describing negative covariance in simulation D is similar in form to that found by Faria et al. (2000) in a southern boreal forest but modified so that mean melt energy remains at 10 mm per period and is spatially fixed, whereas Faria's was linked to the remaining distribution of S as snowcover ablated.

Table 1. Characteristics of Snow Ablation Simulations

Simulation	Type	M	S
A	Uniform M, S	Uniform	Uniform
B	Variable S	Uniform	Lognormally distributed CV=0.3
C	Variable M	Normally distributed CV=0.28	Uniform
D	Covariance (M, S)	$M = 0.673\bar{M}\left(1 + 0.5\frac{S_i}{\bar{S}}\right)$	Lognormally distributed CV=0.3
E	Negative Covariance (M, S)	$M = 1.41\bar{M}\left(1 - 0.3\frac{S_i}{\bar{S}}\right)$	Lognormally distributed CV=0.3

Figure 1 shows the cumulative melt energy applied to snow, cumulative ablation per unit area of ground (Fig. 1a), snow-covered area (Fig. 1b) and snow accumulation per unit area of ground (Fig. 1c) for each melt period. In all cases, melt energy and ablation diverge when f_s becomes less than one. Simulation A ablates the even snow-cover evenly following M until S is depleted at which point f_s drops to zero and melt stops in period 5. This is the form used in many hydrological and climatological models but is not observed in nature (Pomeroy et al., 1998).

Simulation B differs significantly from the uniform case in that cumulative A and M diverge early in the melt sequence, SWE declines more slowly and persists beyond period 7 and f_s declines steadily throughout the simulation. The variable S scenario of B has been the recommended form for snow cover depletion curves in the recent literature (e.g. Donald et al., 1995).

Simulation C with variable M provides a gradual divergence between cumulative A and M from mid-way through melt and an ogive-shaped snow-covered area depletion curve. Ablation is completed by period 7. The variable M scenario of simulation C is not as dramatic a departure from the simulation A as is the variable S scenario (simulation B), but the effects are not insignificant and have not previously been examined.

The positive covariance between M and S simulated in D has not been reported in the literature. This covariance accelerates ablation over the simple case of variable S. Snow cover depletion is initially slowed and then accelerated mid-way through melt compared to simulation B. This may be considered a ‘more efficient’ melt than that with only variable S as the higher melt energy is applied where snow is deeper.

The negative covariance in simulation E retards ablation compared to that estimated using a uniform melt (B). This observation is the opposite of that by Faria et al (2000), the difference may be due to the assumption in this implementation that covariance is fixed to the initial distribution of S, whereas Faria et al. linked the covariance to the rank of remaining SWE values. Snow cover depletion is initially accelerated and then retarded in later melt compared to the uniform melt case. One can argue that the negative covariance melt is ‘inefficient’ in that larger values of melt energy are applied to shallow snow that is soon depleted. The apparent efficiency or inefficiency of simulations D and E are caused by the distribution of melt energy being fixed with respect to location under the canopy, in Faria’s study the distribution was in fact found to be tied to the changing S distribution.

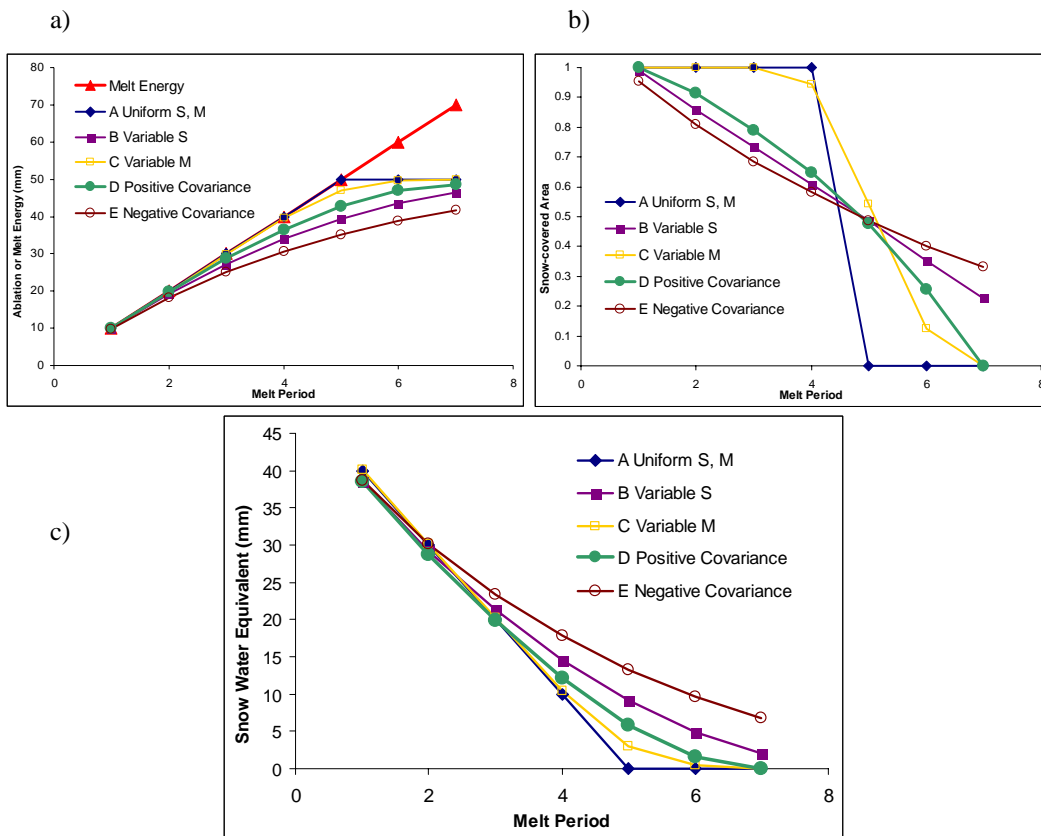


Figure 1. Melt simulations for five scenarios: a) melt energy per unit area of snow and ablation per unit area of ground, b) snow covered area, c) remaining snow water equivalent per unit area of ground.

FIELD METHODS

A snow survey transect was established in a dense, mature white spruce stand (height = 15 m) in at 750 m elevation in Wolf Creek Research Basin (lat. 61 °N), southeast of Whitehorse, Yukon Territory (Janowicz, 1999). The stand has been protected from forest fires and harvesting and so is older than typical in this region. The transect followed a random, 'wandering' path through the forest of approximately 125 m length. Depth stations were located approximately every metre along the transect with density stations every 5 m. Depth was measured with a metal ruler and density with a Mt. Rose style metric snow density tube and scale. Depth and density were measured daily during rapid melt. Measurements were taken at exactly the same spot and in the same order so that values could be associated with a location. Snow water equivalent was calculated from depth and density following Pomeroy and Gray (1995).

RESULTS

Forest snow ablation started on 11 April 1999, but subsequent cold periods and snowfalls made distinction of a clear snowmelt period difficult. An unequivocal melt period began on 18 April during which f_s declined from 1.0 to 0.5 over six days and snow cover was completely depleted in the subsequent three days. Five snow surveys were conducted during this period with an observation of complete snow depletion at the end. Measured snow water equivalent was taken as S and M was only calculated as $S_t - S_{t-1}$ at sites where $S_x > 0$. Mean S included both snow and non-snow covered sites but mean M was only calculated per unit area of sites with $S_x > 0$. All change in snow mass was assumed due to melt and daily change in liquid water storage in these shallow snowpacks was considered negligible.

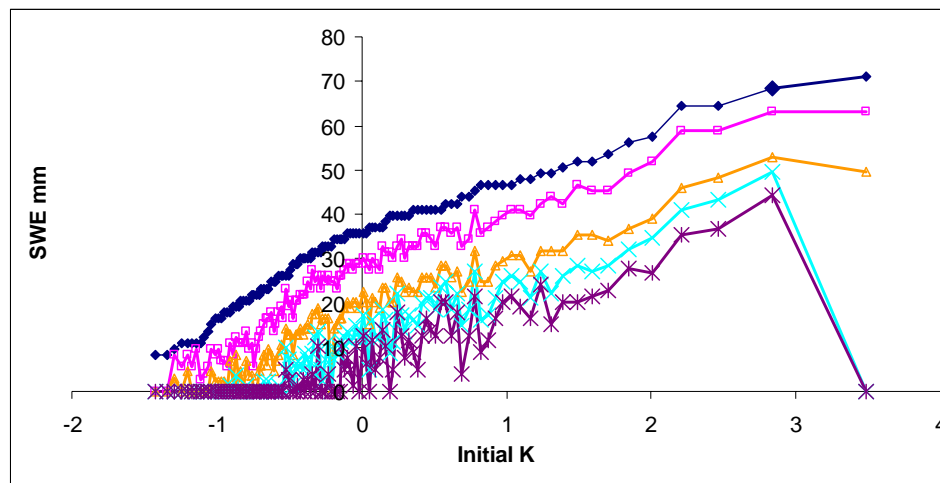


Figure 2. Measured distributions of snow accumulation (18, 19, 20, 21, 23 April 1999) during melt plotted against the frequency factor, K , of the lognormal distribution, derived from the initial distribution.

The initial measured S values can be fitted to the lognormal function (deviation afterwards is expected). Figure 2 shows measured S from the five surveys plotted against the frequency factor K associated with the 18 April S distribution (mean and CV listed in Table 2). Subsequent S values are associated with the K not by assuming that they maintain constant rank (as did Faria et al. 2000), but by registering each measurement to a known survey point. Figure 2 shows that the initial S distribution progressively scatters during melt from the initial lognormal fit and that survey points do not maintain their initial rank of S as melt progresses. However it is difficult to discern any change in slope to the relationship. Figure 3 confirms that, in contrast to Faria et al.s (2000) findings in the southern boreal forest, none of the daily distributions of M are associated

with the initial S distribution. The melt energy and snow accumulation measurements shown in Figs. 2 and 3 suggest that there is

- a) little covariance between M and S
- b) notable variation in M.

The statistical descriptions in Table 2 show that M has a mean coefficient of variation of 0.28 with little variation about this through melt and that S has a coefficient of variation of 0.4 that increases through melt.

Table 2. Statistical Properties of snow accumulation and melt energy

Date	\bar{S}	CV of S	\bar{M}	CV of M
18 April	33	0.41	–	–
19 April	25	0.55	7.6	0.30
20 April	17	0.73	8.8	0.23
21 April	11	1.01	6.7	0.29
23 April	7	1.37	5.6	0.32

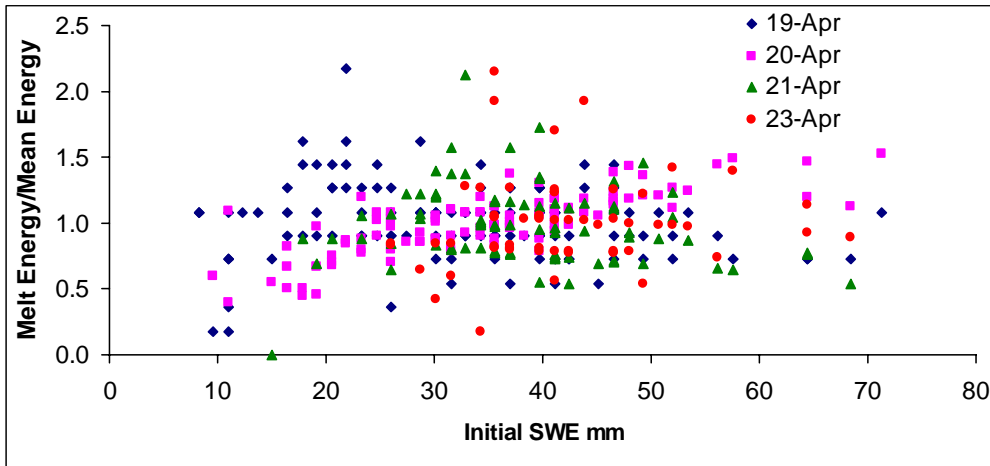


Figure 3. Normalised melt energy for each day plotted against initial snow accumulation (18 April). There is no association between the two (weakly on 20th) and the melt energy changes pattern for each day.

There are no published descriptions of the statistical variation of melt energy at small scales. Given the similar standard deviations of normalised melt energy for each day of melt, the measurements were grouped for further analysis. The distribution of melt energy was also compared to two parameter gamma and lognormal frequency functions but the best fit was to the normal density function. Figure 4 shows the observed normalised melt energy frequency (for 11 classes of melt energy) and the normal probability mass function from the observed normalised mean (1.0) and standard deviation (0.28). The concurrence is excellent.

An unexpected result is that the correlations between observations of melt from day to day were very small ($r < 0.05$) for all sets of observations. This means that the spatial patterns of M were not consistent over time. The physical reasoning behind this is not yet clear, however mixtures of cloudy and clear periods, windy and calm and changing snow edge distances would influence the melt energy available from day to day. It is also possible that the low solar angles during April melt at 61° N meant that most radiation penetration through the dense spruce canopy was via scattering and hence diffuse rather than direct, so that distinctive patterns in openings were less apparent. In a more open subarctic woodland persistent melt patterns would be expected to form and have been observed in Wolf Creek (Woo and Giesbrecht, 2000).

The mean values of cumulative A, cumulative M, S, and f_s as observed and calculated are shown in Fig. 5. The form of deviation in cumulative ablation and melt energy curves is similar to that obtained synthetically from a variable S however the measured range is more limited than those that were modelled. The M and A values for the last melt sequence differ by a factor of 2 however. By the time f_s declined to 0.5, S was less than $1/4^{\text{th}}$ of its value when snow cover depletion began.

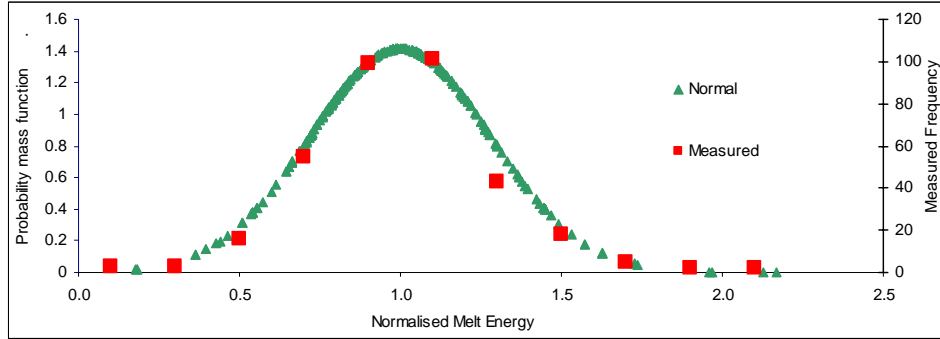


Figure 4. Measured frequency of normalised (divided by mean) melt energy observations ($n=347$) in various classes of melt energy and the probability mass function of a normal distribution having the same standard deviation and mean as the measurements.

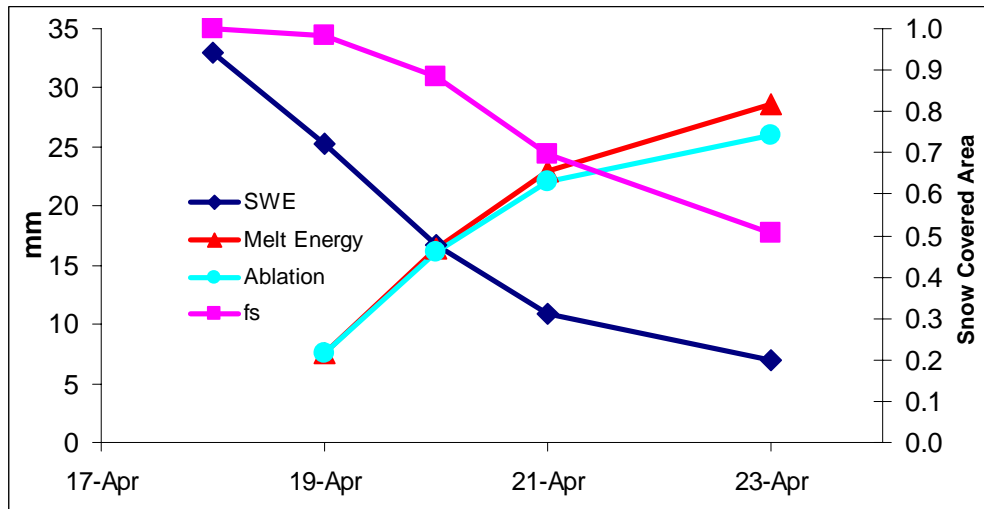


Figure 5. Measured remaining snow accumulation (SWE), melt energy (change to SWE per unit area of snow), ablation (change to SWE per unit area of ground) and snow covered area f_s , Spruce forest, Wolf Creek, Yukon Territory, April 1999.

SIMULATIONS OF ABLATION

In an attempt to simulate the average conditions in Fig. 5 from the techniques outlined, a synthetic series of S_i values was created using the lognormal distribution (Eq. 3) and the measured statistical properties of S_i (Table 2, 18 April). This distribution was ablated in two manners, the first applied uniform melt energy at the mean measured value for each day of simulation. The second created a synthetic series of normally distributed M values that were randomly apportioned to the lognormal distribution of S values for each day of melt. The M values for a particular day had the measured mean for that day and bulk statistical properties ($CV=0.28$) as measured (Table 2). In comparison to measurements, the results show a reasonable match using both techniques. Adding the variable melt energy to the simulation provided little change from that calculated using

only variable snow accumulation; estimates of f_s were improved slightly and those of S degraded slightly.

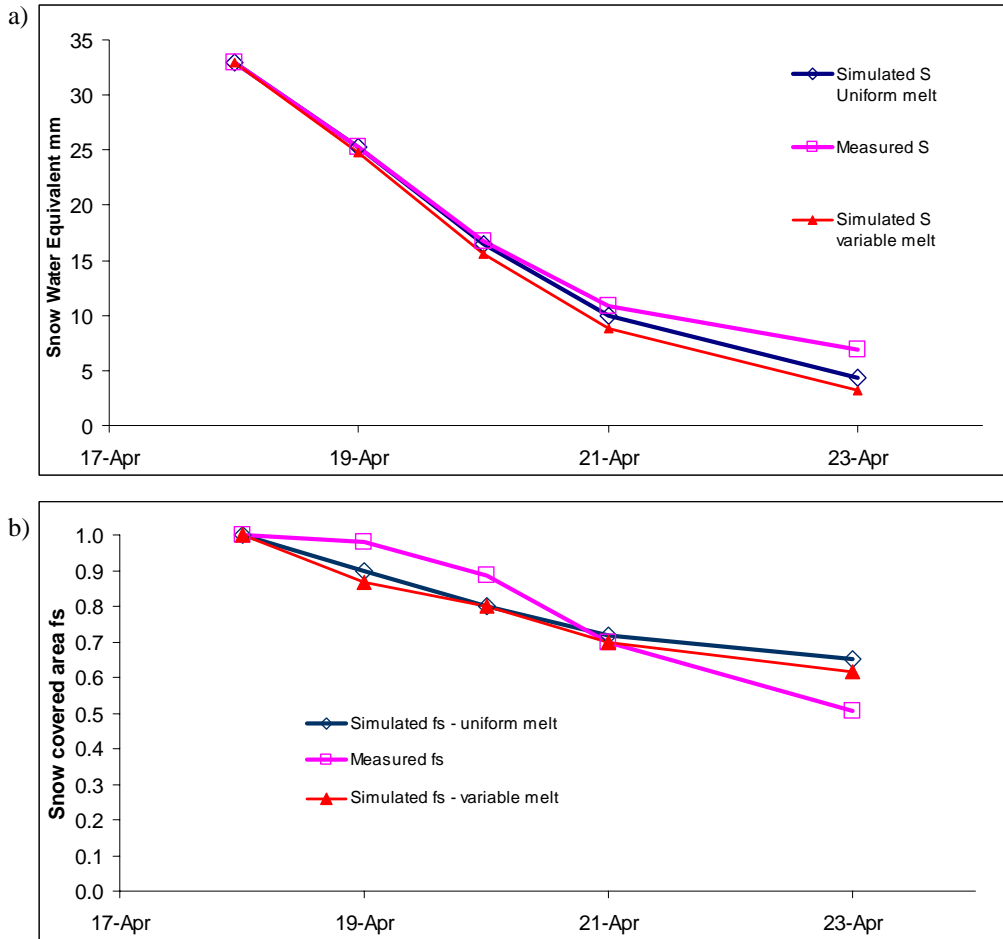


Figure 6. Measurements and simulations of snow ablation and snow cover depletion. Simulations: uniform melt used a synthetic lognormal distribution of S_i and applied mean melt energy; variable melt used the same distribution of S_i and randomly applied a normal distribution of melt energy each day.
a) snow accumulation remaining, b) snow covered area.

DISCUSSION AND CONCLUSIONS

The decrease in snow-covered area observed at larger scales during melt can be caused by small-scale spatial variability in snow accumulation, snowmelt energy or a combination of the two. Theoretical considerations of the effects of variable snow accumulation, variable melt energy and covariance between the two show that spatial variations in snow accumulation and melt energy can work independently to increase the cumulative difference between melt energy applied to snow and ablation by decreasing the snow covered area. A positive spatial covariance between melt energy and initial accumulation accelerates ablation while a negative covariance retards it in comparison to variable snow accumulation effects in isolation.

In a northern, dense, mature spruce forest no spatial covariance between melt energy and initial snow accumulation was found. However, both initial snow accumulation ($CV = 0.4$) and melt energy ($CV = 0.28$) varied substantially over space. The initial snow accumulation distribution was fitted to a lognormal distribution while the melt energy distribution fitted a normal distribution. Distributed simulations of remaining snow accumulation and snow-covered

area during melt using synthetic spatial distributions of accumulation and melt energy with statistical properties identical to those measured showed good fit to measurements, however simulations using a spatial distribution of initial accumulation and uniform melt energy proved equally good. Though the distribution of melt energy in this case of a dense northern spruce forest had an insignificant effect on ablation rates and snow cover depletion, theoretical considerations suggest that melt energy spatial variation can exert a control on ablation rates and that observed snow cover depletion curves should not be wholly ascribed to variations in initial snow accumulation.

ACKNOWLEDGEMENTS

This research was funded in Canada by MAGS (Mackenzie Global Energy and Water Cycling Experiment Study) through the National Water Research Institute, Environment Canada and the Natural Sciences and Engineering Research Council of Canada and in the UK by the Natural Environment Research Council through grant NER/M/S/2000/00287 'Representation of snow ablation processes for land surface schemes'. The assistance of Newell Hedstrom (NWRI) and Dell Bayne (Univ. of Saskatchewan) with all aspects of fieldwork, and the hospitality and support of Wolf Creek Research Basin by Richard Janowicz (Water Resources Division, Indian and Northern Affairs Canada, Whitehorse, Yukon) are gratefully acknowledged. Enjoyable discussions on the topic with Don Gray, Kevin Shook and Richard Essery promoted this study.

REFERENCES

- Buttle, J.M. and J.J. McDonnell, 1987. Modelling the areal depletion of snowcover in a forested catchment. *Journal of Hydrology*, 90, 43–60.
- Davis, R. E., Hardy, J. P., Ni, W., Woodcock, C., McKenzie, J. C., Jordan, R. and Li, X. 1997. "Variation of snow cover ablation in the boreal forest: A sensitivity study on the effects of conifer canopy", *Journal of Geophysical Research*, **102**, 29389–29395.
- Donald, J.R., E. D. Soulis, N. Kouwen and A. Pietroniro 1995. A land cover-based snow cover representation for distributed hydrological models. *Water Resources Research*, 31(4), 995–1009.
- Faria, D.A., Pomeroy, J.W. and R.L.H. Essery, 2000. Effect of covariance between ablation and snow water equivalent on depletion of snow-covered area in a forest. *Hydrological Processes*, 14, 2683–2695.
- Golding, D. L. and Swanson, R. H. 1986. "Snow distribution patterns in clearings and adjacent forest", *Water Resources Research*, **22**, 1931–1940.
- Hardy, J.P., Melloh, R., Robinson, P. and R. Jordan, 2000. Incorporating effects of forest litter in a snow process model. *Hydrological Processes*, 14, 3227–3237.
- Janowicz, J.R. 1999. Wolf Creek Research Basin: an overview. In, (eds. J. Pomeroy and R. Granger) *Wolf Creek Research Basin: Hydrology, Ecology, Environment*. Environment Canada, National Water Research Institute. 121–130.
- Jones, H.G. 1987. "Chemical dynamics of snowcover and snowmelt in a boreal forest", In, (eds. H.G. Jones and W.J. Orville-Thomas) *Seasonal Snowcovers: Physics, Chemistry, Hydrology*, NATO ASI Series C211. Reidel, Dordrecht, Holland. 531–574.
- Pomeroy, J.W. and D.M. Gray, 1995. *Snow Accumulation, Relocation and Management*. NHRI Science Report No. 7. Environment Canada, 144p. (available from Natl. Water Res. Inst., Saskatoon)
- Pomeroy, J. W., Gray, D. M., Shook, K. R., Toth, B., Essery, R. L. H., Pietroniro, A. and Hedstrom, N. 1998. "An evaluation of snow accumulation and ablation processes for land surface modelling", *Hydrological Processes*, **12**, 2339–2367.
- Shook, K. 1995. *Simulation of the Ablation of Prairie Snowcovers*, Ph.D. thesis, Department of Agricultural and Bioresource Engineering, University of Saskatchewan, Saskatoon, Saskatchewan, Canada, p. 189.

- Shook, K. and Gray, D. M. 1997. "Snowmelt resulting from advection", *Hydrological Processes*, **11**, 1725–1736.
- Sturm, M. 1992. "Snow distribution and heat flow in the taiga", *Arctic and Alpine Research*, **24**, 145–152.
- Verry, E. S., Lewis, J. R. and Brooks, K. N. 1983. "Aspen clearcutting increases snowmelt and storm flow peaks in north central Minnesota", *Water Resources Bulletin*, **19**, 59–67.
- Woo, M. and Steer, P. 1986. "Monte Carlo simulation of snow depth in a forest", *Water Resources Research*, **22**, 864–868.
- Woo, M. and M.A. Giebrecht, 2000. Simulation of snowmelt in a subarctic spruce woodland: 1. Tree model. *Water Resources Research*, 36(8), 2275–2285.